







Influence of citric acid on the fire behavior of gypsum coatings of construction and structural elements

 F.J. Castellón ^a ,  M. Ayala ^a,  J.A. Flores ^b,  M. Lanzón ^c

a. Department of Structures, Construction and Graphic Expression, Technical University of Cartagena, (Murcia, Spain)

b. Department of engineering, Miguel Hernández University, (Alicante, Spain)

c. Department of Architecture and Building Technology, Technical University of Cartagena, (Murcia, Spain)

 franciscojose.castellon@upct.es

Received 20 October 2020

Accepted 21 January 2021

Available on line 04 June 2021

ABSTRACT: To improve the workability in gypsum plasters, additives are sometimes used, including citric acid, which provides acceptable setting times for low w/g ratios, maximizing the mechanical properties of the material. The influence of citric acid on the fire response of gypsum coatings is not well known, and so our aim was to analyze the effects that citric acid produces on the behavior of gypsum plasters exposed to fire. Temperature measurements were made with sensors and thermal imaging cameras while other instrumental techniques, including SEM, XRD and TG, were used to characterize the microstructure and composition of gypsum materials subjected to the action of fire. The fire had a greater effect on gypsum plasters containing citric acid as revealed by the cracking patterns and heat propagation profiles observed. Likewise, micro-cracks were observed in gypsum specimens, containing and non-containing citric acid, exposed to fire. In all cases, the alterations were consistent with the temperature profiles and chemical composition of the faces whether exposed to fire or not.

KEYWORDS: Gypsum; Citric acid; Fire; Temperature; Passive protection.

Citation/Citar como: Castellón, F.J.; Ayala, M.; Flores, J.A.; Lanzón, M. (2021) Influence of citric acid on the fire behavior of gypsum coatings of construction and structural elements. *Mater. Construcc.* 71 [342], e248. <https://doi.org/10.3989/mc.2021.13120>.

RESUMEN: *Influencia del ácido cítrico en el comportamiento al fuego de revestimientos de yeso de elementos constructivos y estructurales.* Habitualmente, para mejorar la trabajabilidad del yeso se utilizan aditivos, entre ellos el ácido cítrico, que proporciona tiempos de fraguado aceptables para relaciones a/y bajas, potenciando al máximo las propiedades mecánicas de este material. La influencia del ácido cítrico en la respuesta frente al fuego de revestimientos de yeso no se conoce bien. El objetivo de este trabajo consiste en analizar los efectos que produce el ácido cítrico en el comportamiento frente al fuego del yeso. Para ello se usaron medidas de temperatura con sensores, cámara termográfica y otras técnicas instrumentales (SEM, XRD y TG) para caracterizar la microestructura y composición de los materiales de yeso sometidos a la acción del fuego. El fuego tuvo mayor efecto en yesos que contienen ácido cítrico, tal como revelaron los patrones de fisuración y los perfiles de propagación de calor obtenidos. Asimismo, se apreció formación de micro-fisuras en probetas de yeso aditivadas con ácido cítrico y sin aditivar, expuestas a fuego. En todo caso, la manifestación de las alteraciones fue coherente con los perfiles de temperatura y composición química de la cara expuesta y no expuesta al fuego.

PALABRAS CLAVE: Yeso; Ácido cítrico; Fuego; Temperatura; Protección pasiva.

Copyright: ©2021 CSIC. This is an open-access article distributed under the terms of the Creative Commons Attribution 4.0 International (CC BY 4.0) License.

1. INTRODUCTION

Fire regulations require that construction and structural elements reduce to acceptable limits the risk for the users of a building that suffers damage in the face of a fire of accidental origin (1). Therefore, a better knowledge of the fire behavior of the construction materials is essential to ensure this basic requirement.

For many centuries, gypsum has been widely used in construction because, among other reasons, it is an inexpensive and abundant material. In addition, it is one of the most environmentally acceptable binders because it requires relatively low firing temperatures to obtain the hydraulically active form (basanite or calcium sulphate hemihydrate). Gypsum plasters offer important features as easy installation and finishing (workability), good thermal insulation and, above all, suitable behavior against fire due to its ability to absorb a considerable amount of energy. In fire events, part of the energy is used to evaporate a significant amount of crystallization water from $\text{CaSO}_4 \cdot 2\text{H}_2\text{O}$, thereby preventing the energy from contributing to increasing the temperature. (2).

The first scientific results on the thermal behavior of gypsum did not appear until the middle of the 20th century (3, 4). At this time too, the first fire tests on gypsum plasters were carried out, becoming the first comparisons with other types of construction materials (aerated concrete or cement mortar, among others) (2), even the first studies using perlite, vermiculite and sand are reported in the literature (5). From this moment, research has continued into the behavior of both pure gypsum (6) and different gypsum compounds used as fire protection materials (7). While many recent studies have focused on laminated gypsum board because of its widespread presence in the construction sector (8-13), new gypsum-based composite materials have also been studied (14, 15).

Time-temperature curves (normalized fires) are used to study the fire behavior of many materials, measuring the temperature of the air in the proximity of the surfaces of an element as a function of time. The Technical Building Code (1) includes the normalized time-temperature curve defined in the UNE-EN 1363-1 standard (16), which has been referenced in numerous studies on the fire behavior of construction materials (17- 20).

In this standard the following equation represents the theoretical fire (Equation [1]):

$$\theta_g = 20 + 345 \log_{10} (8t + 1) \text{ (}^\circ\text{C)} \quad [1]$$

where θ_g is the gas temperature on the surface exposed to fire ($^\circ\text{C}$), and t is time elapsing since the fire started (min).

One of the main features of gypsum is that it sets very quickly, which considerably limits its workability: the lower the w/g ratio, the higher the mechanical properties, but the lower the workability and open

time. To solve this problem several types of retarders, such as polycarboxylic acids and more specifically, citric acid are used in gypsum plasters. Numerous studies have been published on the influence of citric acid as an additive in gypsum, mainly focusing on its influence on the microstructure (21-23), mechanical properties (23, 24), and, especially, its workability (23, 25, 26). Citric acid has a considerable influence on the microstructure of gypsum and changes its microstructure. As the dose of citric acid increases, the morphology is altered from one of acicular crystals with a high degree of crosslinking to thicker and relatively independent prismatic crystals at high doses. Indeed recent studies have confirmed that as the dose of citric acid increases, so the mechanical properties of the gypsum decrease and its workability increases, starting to set after about 50 min for doses equal to or greater than 500 ppm (23), although other works report that when the citric acid dose is small the mechanical properties can be improved (25).

However, the influence of citric acid on the fire behavior of gypsum is not well known, and, although several studies report on practical properties as workability, setting and open time of plasters, the influence of citric acid on the response of gypsum to fire has received less attention (7, 17). The objective of this work, therefore, was to analyze the influence of citric acid on gypsum plasters, especially the thermal characteristics, microstructure and integrity, and to compare the results obtained with the behavior of plasters without additives for different w/g ratios.

2. EXPERIMENTAL PROCEDURE

2.1. Materials

2.1.1. Gypsum

The commercial gypsum used in the study ($\text{CaSO}_4 \cdot \frac{1}{2}\text{H}_2\text{O}$) was supplied by a local manufacturer, and is a construction plaster classified as B1 according standard EN 13279-1 which establishes the characteristics that construction plasters must meet (27).

2.1.2. Additives

Citric acid was used as a setting retarding additive. As regards the time at which it should begin to set, the norm indicates that for manual application it must be greater than 20 minutes and greater than 50 minutes for mechanical application.

Gypsum specimens without additives were made up with w/g ratios of 0.4 and 0.7. W/g ratios in the order of 0.4 are common in commercial gypsum products. This ratio provides gypsums with high mechanical resistance, but excessively short workability times. For this reason, citric acid concentrations

were varied until a setting start time of around 50 min was achieved, while the different doses were tested by studying the workability of each blend. The citric acid dose that led to an open time of around 50 min was 600 ppm (0.6 g of additive per kg of gypsum).

2.2. Methods

2.2.1. Preparation of specimens

The standard EN 13279-1 covers the general definitions and requirements made for gypsum plasters (27). Regular water was used to prepare the mixtures, and the knife method was used to determine the setting times. This method measures the time elapsing before a knife cut made in the surface of the paste ceases to heal (28).

Gypsum specimens were made with the following dimensions; 200 mm x 200 mm x 20 mm with w/g ratios of 0.4 and 0.7. In addition, 0.4 w/g specimens were made to which 0.6 g of citric acid was added per kg of gypsum (0.4 w/g + 0.6 g/kg C. A.) (Figure 1).

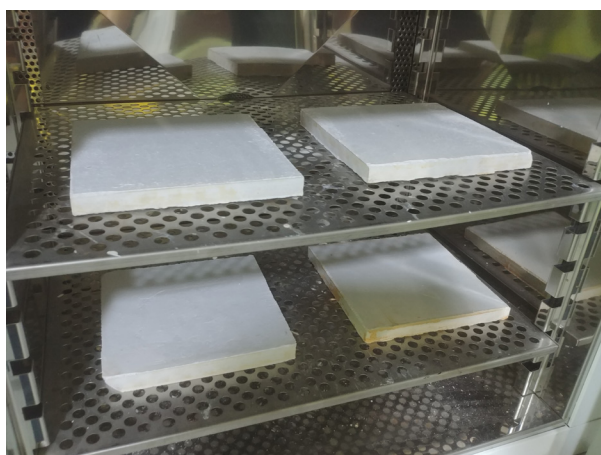


FIGURE 1. Specimens in oven.

The specimens were cured for 90 days in a laboratory environment (23 ± 3 °C y $55 \pm 10\%$ HR). Before carrying out the tests, the specimens were kept in an oven at a temperature of 40 °C until the mass was constant.

2.2.2. Fire test

The specimens were exposed to direct fire using a blow torch fed by propane gas, anchored to a mobile support with a graduated path, which was gradually moved from position 0 to position 5, and remained in each position for 2, 3, 4, 5, 6 and 10 minutes respectively. Through this procedure it was possible to vary the temperature reached in the exposed face (EF) from room temperature to approximately 800 °C.

At the same time, images of the specimen surface not exposed to fire were obtained by thermographic camera in order to analyze both the temperature and the heat distribution. For this, the specimens were placed on a stainless steel support and the fire protocol described above was applied, performing 30 minutes tests in which a thermal image was recorded every minute using a FLIR T400 camera attached to a tripod in fixed position (Figure 2).

In addition, the temperature of the fire was measured on the exposed face by means of a chromel-alumel K type thermocouple located in the action center of the flame. In this case, thermographic measurement could not be used because the heat from the flame saturates the camera detector and is not capable of measuring the temperatures reached on the fire-exposed face. An Omron ZR-RX 25 Data Logger was used to record the temperature measurements made by the thermocouple.

2.2.3. Scanning electron microscope (SEM) analysis

SEM images were obtained from the untested gypsum samples and the samples that had been exposed

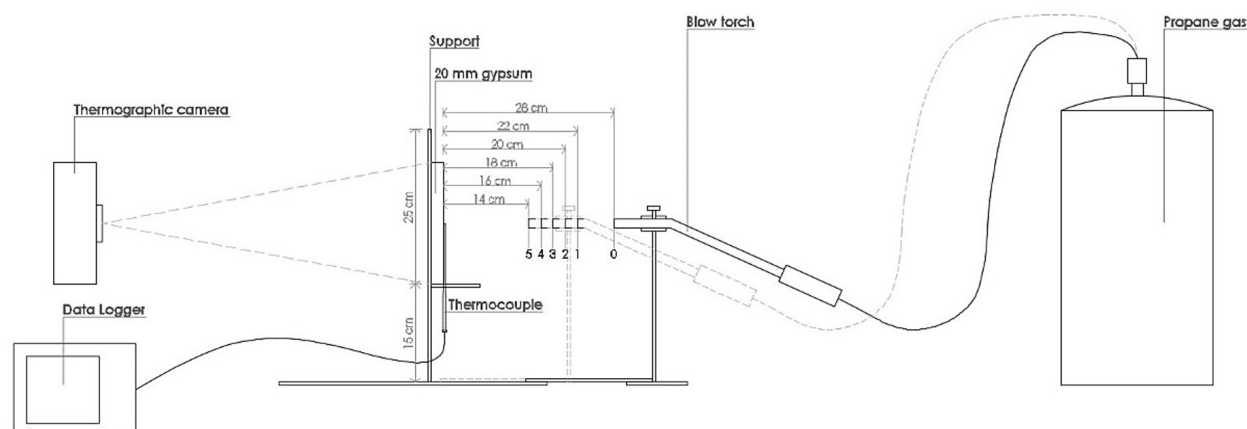


FIGURE 2. Diagram of the direct fire test components.

to fire, in which case both the exposed face (EF) and non-exposed face (NEF) were recorded, using a Hitachi S-3500N scanning electron microscope. The SEM observation was made at a voltage of 15 kV and 2000 magnification using Backscattered Electrons (BSE).

2.2.4. X-ray diffraction (XRD)

The gypsum powder samples, the non-fire tested gypsum and the fire tested samples corresponding to the exposed face (EF) and the non-exposed face (NEF) were subjected to XRD analysis, which provided important chemical information about the mineral phases present since they are sensitive to temperature. The samples were gently ground in a mortar and the mineral phases were identified using the Cu K-alpha line using a Bruker D8 Advance powder diffractometer for powder analysis. A scan angle range (2-theta) of 10° to 70° with a resolution of 0.05° was used.

2.2.5. Thermal analysis by Thermogravimetry (TG)

The powdered gypsum samples of the non-tested gypsum and the two samples corresponding to the exposed face (EF) and the non-exposed face (NEF) were studied by thermogravimetric TG analysis, which measures the variation in mass of a specimen as a function of temperature or time. For this, a Mettler-Toledo TGA / DSC HT thermogravimetric analyzer was used, whose horizontal oven has a temperature range running from room temperature to 1600 °C with an accuracy of ± 0.5 °C used with a heating rate of 20 °C / min. N₂ at a flow rate of 20 ml / min and O₂ at 50 ml / min were used in the oven atmosphere.

A metal blade was used to take the samples, with which the most superficial layer of the samples was eroded. The amount of sample per test used was approximately 10 mg.

3. RESULTS AND DISCUSSION

3.1. Characterization of the binder: XRD, XRF and TG

A previous XRD study carried out on the powdered gypsum confirmed the presence of bassanite (CaSO₄·½H₂O) as the main mineral phase with a much lower presence of anhydrite or anhydrous calcium sulfate (CaSO₄), calcite (CaCO₃) and dolomite (CaMg(CO₃)₂) (Figure 3). The very low level of gypsum dihydrate detected among its minor components would have been due to the natural hydration of the binder with ambient water vapor.

Gypsum powder was also studied by TG. A first mass loss of 4.88% was obtained corresponding to the transformation of calcium sulfate hemihydrate (CaSO₄·½H₂O) into anhydrite (CaSO₄) at around 130 °C. Subsequently, at a temperature of approximately 670 °C, a second mass loss of 2.49% was observed, again due to the decarbonation of calcite (CaCO₃) accompanied by a loss of CO₂ (CaO + CO₂) (Figure 4).

Finally, a study of the material was carried out using XRF, from which the percentage concentration of the elements that make up the gypsum expressed in the form of oxides was obtained (Table 1). As expected, the two major oxides were those associated with the elements Ca and S. The H₂O and CO₂ data were not determined by XRF but obtained from TG since this technique has great-

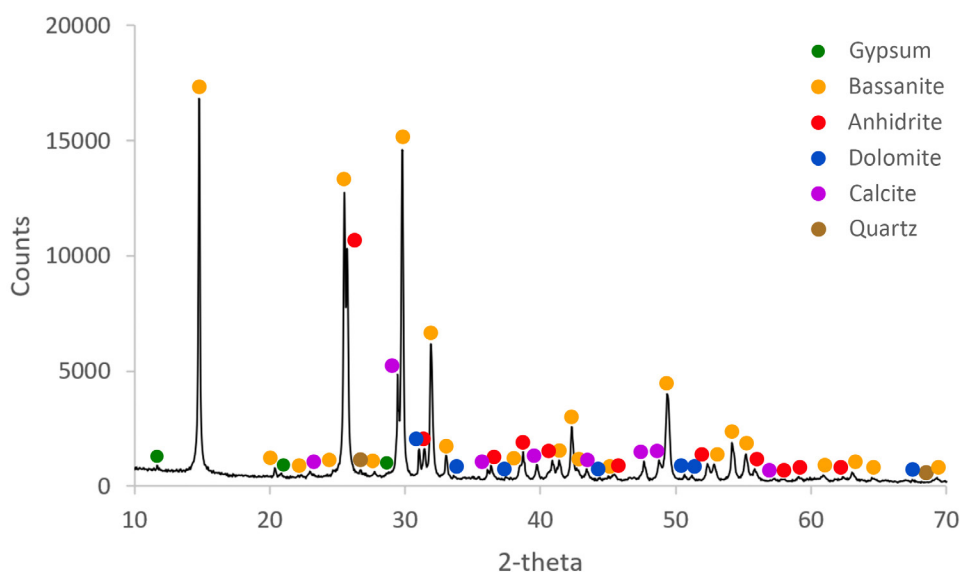


FIGURE 3. XRD of Binder B1.

er sensitivity and reliability for detecting elements with low atomic number due to their low X-ray absorption.

3.2. Fire tests

Once set and cured, the heat transfer of the tested plasters increases with their density (27), as was confirmed by apparent density measurements. The 0.4 w/g and 0.7 w/g mixtures provided apparent densities of 1.472 g/cm³ and 1.034 g/cm³, respectively. Gypsum 0.4 w/g is denser than gypsum 0.7 w/g. The temperatures recorded during the test for the 0.4 w/g ratio were higher than those recorded for the 0.7 w/g ratio, except in the final period from minute 28 onwards, when slightly higher temperatures were recorded for the 0.7 w/g ratio, although the mean temperature was still lower (Figure 5). The greater porosity of the gypsum at 0.7 w/g probably produced a greater long-term alteration (> 28 min) as a result of exposure to direct fire, thus increasing the diffusion of heat in the final portion of the test from the exposed face to the non-exposed.

TABLE 1. XRF of Binder B1.

Oxide	Concentration (%)
	Binder B1
H ₂ O*	4.8772
CO ₂ *	2.4943
MgO	0.80
Al ₂ O ₃	0.38
SiO ₂	1.19
SO ₃	49.10
K ₂ O	0.16
CaO	40.47
TiO ₂	0.02
Fe ₂ O ₃	0.19
SrO	0.23
Other	0.09

*: H₂O and CO₂ were determined by TG.

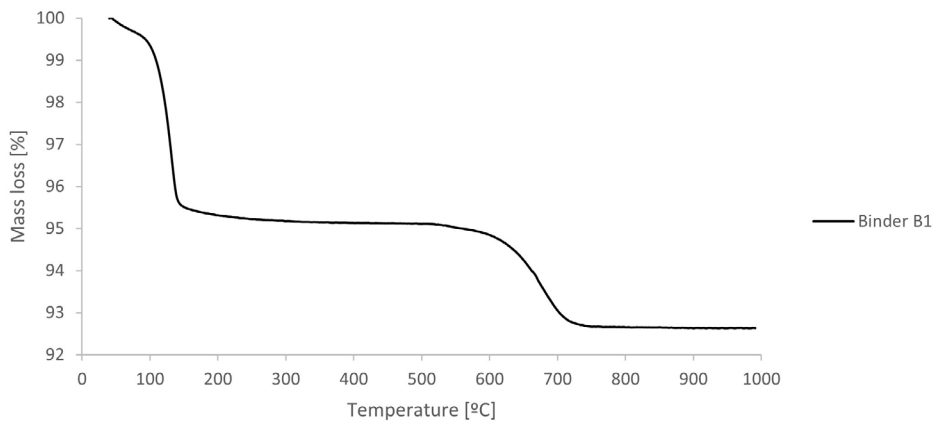


FIGURE 4. TG of Binder B1.

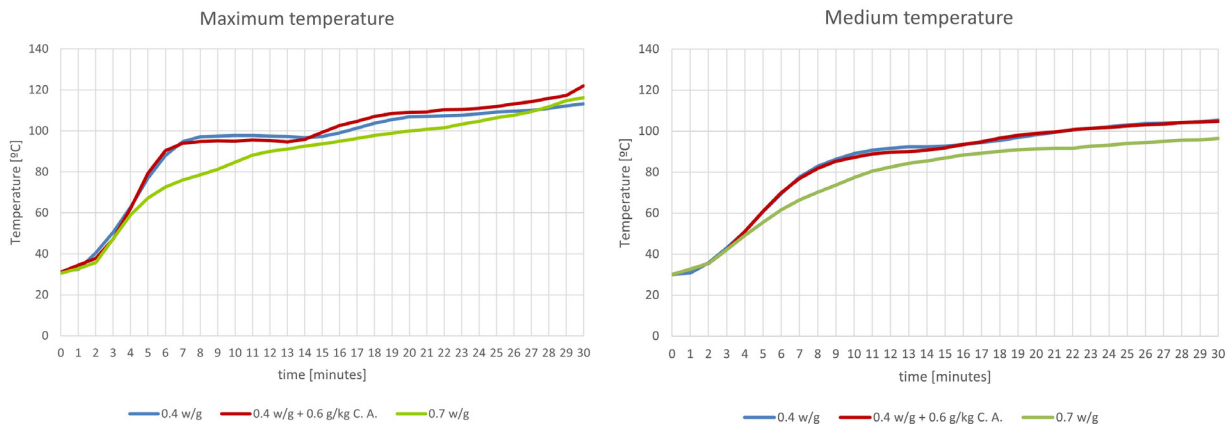


FIGURE 5. Temperatures recorded on the NEF.

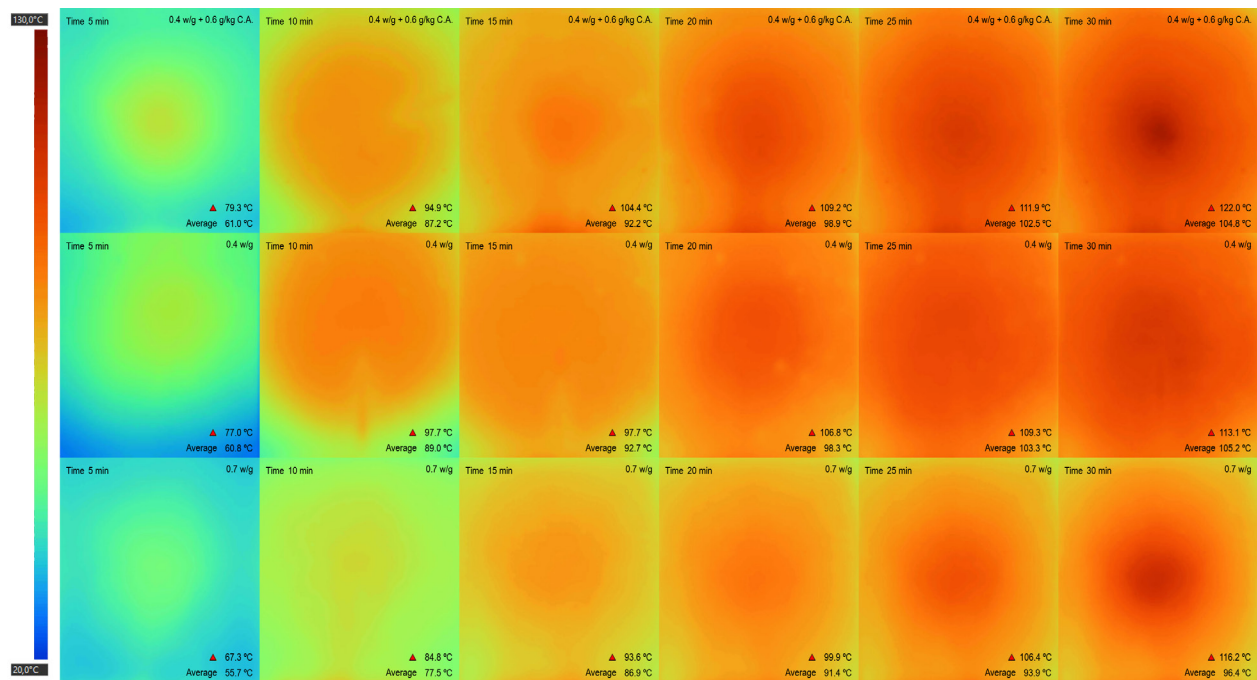


FIGURE 6. Temperatures recorded on the NEF.

If the results obtained for the ratios 0.4 w/g and 0.4 w/g + 0.6 g/kg C. A. are compared, it can be seen that up to about minute 7 both the maximum and mean temperatures increased at a similar rate. From that moment onwards, the slope flattens out substantially in both, corresponding to the evaporation of part of the crystallization water of the gypsum. This plateau lasted about 2 minutes less in the samples containing citric acid, indicating that the generation of $\text{CaSO}_4 \cdot 2\text{H}_2\text{O}$ by hydration of $\text{CaSO}_4 \cdot \frac{1}{2}\text{H}_2\text{O}$ was hampered in the presence of citric acid, as demonstrated in recent studies (23). At about minute 14 of the test, the maximum temperatures recorded in the specimens containing citric acid were higher than those recorded in the gypsum specimens without additives.

However, the average temperatures obtained throughout the test were very similar. Three tests per dosage were performed, confirming the trends described and the consistency of the measurements (Figure 5).

Figure 6 shows a selection of the images obtained with the thermographic camera after 5, 10, 15, 20, 25 and 30 minutes of exposure to fire. The composition of each specimen is shown in the upper right-hand corner of the image, while the bottom right-hand corner shows the maximum temperature as well as the average temperature recorded in the specimen. These images represent a temperature map of the non-fire exposed face of several 2 cm thick gypsum specimens (both with and without additives) that could be used that might be found as materials used for passive protection of other construction and structural elements.

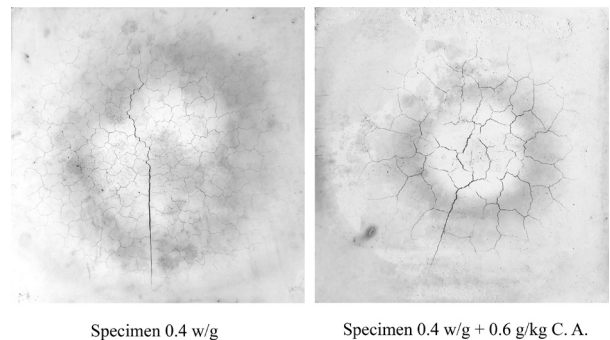
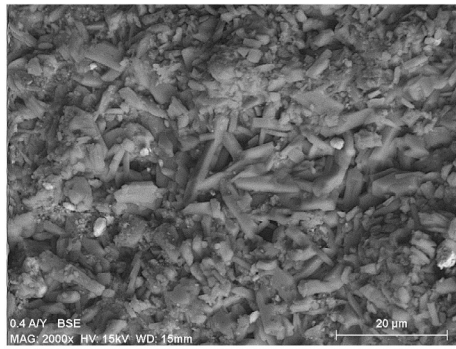


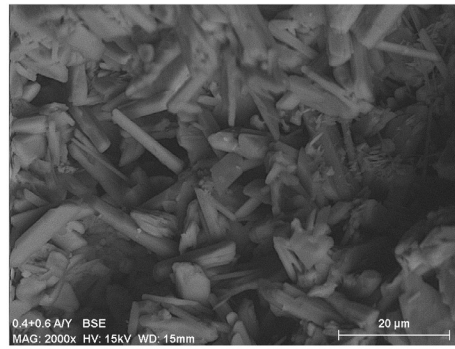
FIGURE 7. Cracking of specimens with the same w/g ratio.

The lowest degree of heat transmission almost throughout the test was that of the 0.7 w/g gypsum board, although during the final few minutes, the temperatures were slightly higher than for the 0.4 w/g ratio probably because its greater porosity led to a greater alteration due to exposure to fire. Little difference was observed between the gypsum with and without added citric acid for the same w/g ratio. For the 0.4 w/g ratio, the temperature peak was lower than for the 0.4 w/g ratio + 0.6 g/kg C. A., but the heat was distributed over a wider area of the specimen, which meant that the average surface temperatures of the specimens were practically similar.

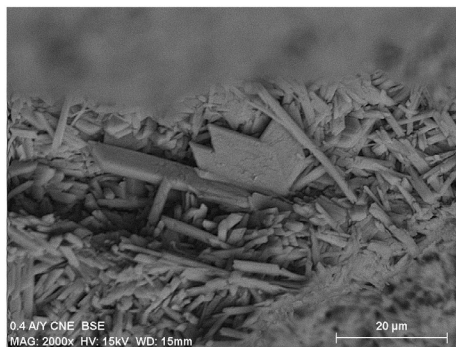
The slightly different behavior of gypsum with added citric acid from the gypsum without additive could be due to the effect of citric acid on the microstructure of gypsum, which would affect the transmission of heat through the plate.



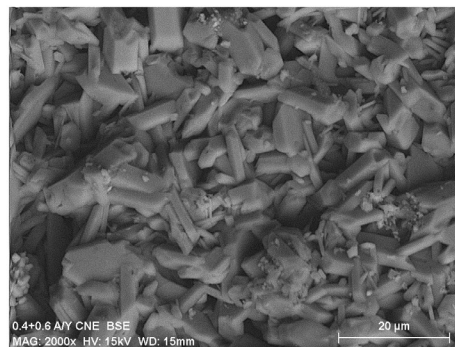
a. Without testing by fire
0.4 w/g



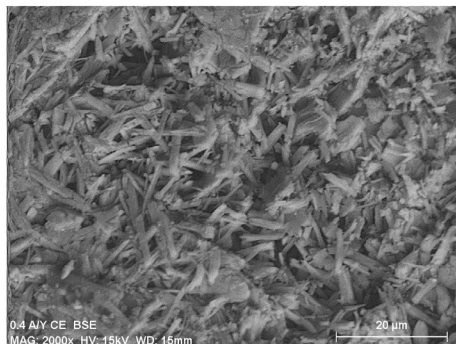
b. Without testing by fire
0.4 w/g + 0.6 g/kg C. A.



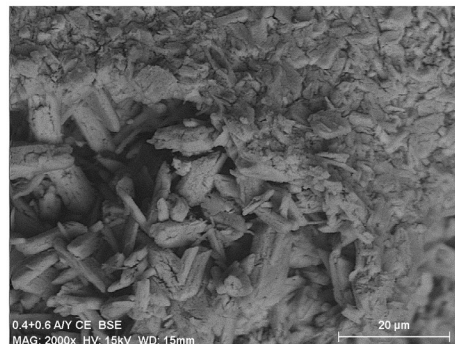
c. 30 min. exposure to fire (NEF)
0.4 w/g



d. 30 min. exposure to fire (NEF)
0.4 w/g + 0.6 g/kg C. A.



e. 30 min. exposure to fire (EF)
0.4 w/g



f. 30 min. exposure to fire (EF)
0.4 w/g + 0.6 g/kg C. A.

FIGURE 8. Images SEM.

Once the 30-minute fire test had finished, photographs of the face that had been exposed to fire (EF) were taken. Figure 7 shows the cracking map of the 0.4 w/g dosed specimen and 0.4 w/g + 0.6 g/kg of citric acid dosed specimen. As can be seen, the cracking pattern differs considerably, and agrees with the heat distribution observed by thermal camera on the surface of the specimen. The specimen containing citric acid had fewer but wider cracks than those that appeared in the specimen

without citric acid. This might also explain why the temperatures were higher in the central zone in the presence of citric acid (due to the greater width of the fissure).

3.3. Scanning electron microscope (SEM) analysis

Figure 8 shows the effect of citric acid on the microstructure of the gypsum samples studied.

As can be seen, citric acid has a strong effect on the gypsum microstructure. The specimens that do not contain citric acid had acicular crystals with twins and crystals behaved differently had a or had crystalline morphologies (Figure 8a). However, in the gypsum with added citric acid, more prismatic shapes and a degree of amorphization of the crystalline framework could be observed (Figure 8b). These results correspond to those already carried out on this subject (22, 23, 29).

After the test, the specimens exposed to fire from both the non-exposed face (NEF) and the exposed face (EF) were observed by scanning electron microscope. As can be seen in Figure 8c and Figure 8d the gypsum crystals of the EF were still perfectly recognizable which agrees with the temperature records obtained by thermal imaging camera since the average temperature did not exceed 110 °C. However, the microstructure of the samples directly exposed to fire (EF) differed from the above (Figure 8e and Figure 8f). In the first place, different crystalline behaviour corresponding to bassanite and anhydrite were observed, since the temperatures recorded with the thermocouple of the EF being around 800 °C and therefore much higher than the complete dehydration of the plaster. In addition, small cracks were observed as a result of the thermal stress of the coatings exposed to direct fire, especially in the samples with added citric acid.

3.4. X-ray diffraction (XRD)

From the analysis of the results obtained, it is clear that, once cured and before being tested by fire, the gypsum is rich in calcium sulfate dihydrate, with small amounts of bassanite and anhydrite, as expected in this type of material (Figure 9a and Figure 9b).

Additional XRD tests were carried out on both faces of the specimens tested by fire, to verify the effect of temperature on the mineral phases described above. On the non-exposed face (NEF), the greater presence of the most hydrated mineral in the series (gypsum) was clearly observed for the sample without citric acid (Figure 10a) compared with the same

sample containing citric acid (Figure 10b). For example, the major peak at low 2-theta angles was substantially reduced by incorporation of citric acid. This may confirm the effect of citric acid on morphological changes (crystal habits) of gypsum (23, 30) leading to more heat-conductive plasters. Finally, it is worth noting that XRD is a semi-quantitative technique and, although the peaks intensities may reveal some differences, this should be confirmed by quantitative methods like TG. As expected from the temperature records on the unexposed face, there were no differences in thermally stable minerals such as quartz or in other minerals that are much more stable than gypsum, such as calcite and dolomite.

However, the results obtained on the exposed face (EF) indicate that after that time of exposure to fire practically all of the gypsum had become anhydrite (Figure 10c and Figure 10d). Neither of the figures show much sign of plaster, which suggests that practically all of the material has been dehydrated as indicated by the SEM images described above. Even thermally stable minerals such as calcite and dolomite, which decompose above 750-800 °C, were almost completely decomposed. Therefore, the XRD studies corroborated that a direct fire scenario produces a thermal stress that considerably alters the microstructure and composition of the coating.

3.5. Thermal analysis by Thermogravimetry (TG)

A thermogravimetric study allows the degree of hydration of gypsum to be based on its resistance and degree of exposure to fire (31). The results of the behavior of specimens not subjected to the fire exposure tests, fire-tested specimens from the non-exposed face (NEF) and fire-tested specimens from the exposed face (EF) are presented below.

In specimens not subjected to fire (Figure 11), the results obtained indicate that in the initial state, the first mass loss occurred at around 150 °C, corresponding to the transformation of gypsum dihydrate ($\text{CaSO}_4 \cdot 2\text{H}_2\text{O}$) to bassanite ($\text{CaSO}_4 \cdot \frac{1}{2}\text{H}_2\text{O}$) and finally anhydrite (CaSO_4). Both processes occurred at

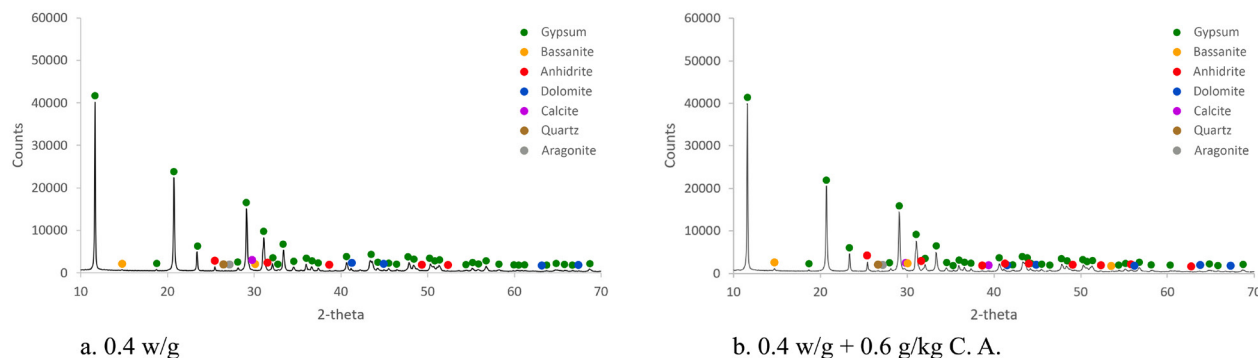


FIGURE 9. XRD specimens not tested on fire.

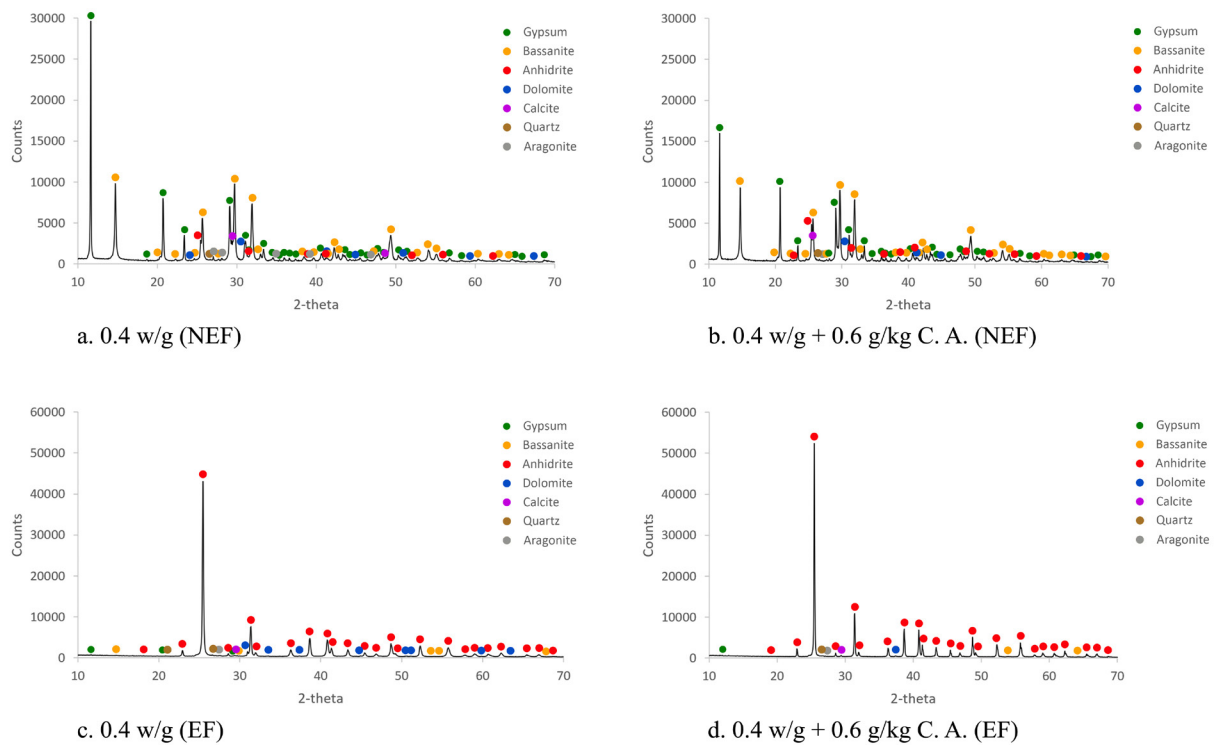


FIGURE 10. XRD fire tested specimens during 30 minutes.

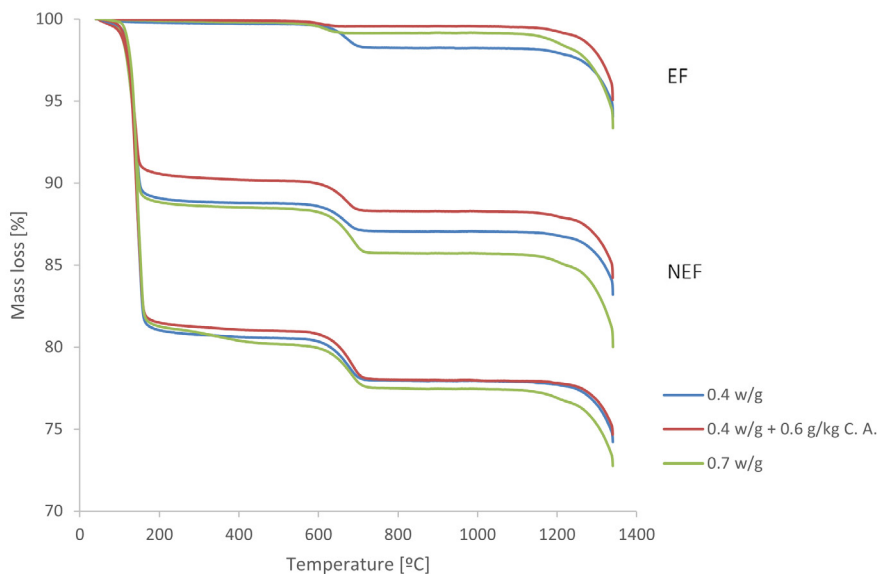


FIGURE 11. TG specimens not tested with fire and tested in fire for 30 minutes (NEF and EF).

temperatures that were very close and were therefore seen as a single water loss process in the thermogram. The first step of the TG curve is due to water crystallization release from $\text{CaSO}_4 \cdot 2\text{H}_2\text{O}$. As can be seen, the weight loss for 0.4 w/g ratio + 0.6 g/kg C.A is lower than that of 0.4 w/g. Taking into account the high sensitivity of TG technique the observed differ-

ence, although minor, may indicate lower formation of $\text{CaSO}_4 \cdot 2\text{H}_2\text{O}$ in the former sample. Finally, the TG results are consistent with the maximum temperature profile found in Figure 5. After 30 min, the maximum temperature recorded on the non-exposed face of samples containing citric acid was higher than that recorded for the remaining ones.

The second and third mass loss in all the thermograms corresponded to the thermal decomposition of carbonates (calcite) into calcium oxide and carbon dioxide at around 650-700 °C and the decomposition of anhydrite sulfate (CaSO_4) in calcium oxide and carbon sulfur dioxide at 1300-1350 °C.

In the thermograms made on specimens from the face not exposed to fire (NEF), after 30 minutes of testing, the three above described steps are also evident (Figure 11). The first loss of mass at about 150 °C corresponding to the loss of water produced by the sequential change from gypsum to bassanite and anhydrite, was considerably lower in the dosage containing citric acid, possibly due to the fact that the additive inhibits the hydration of the bassanite forming less product with as much crystallization water as possible (gypsum).

This result corroborates the analyses obtained for the NEF in the XRD, where more intense diffraction signals of the gypsum mineral were observed for the 0.4 w/g dosage with respect to the same sample with citric acid. There was also a small difference in mass loss between the 0.4 and 0.7 w/g coating which was slightly greater in the latter.

Again, there a second mass loss occurred between 650 and 700 °C due to the thermal decomposition of carbonates (calcite) and a third loss between 1300 and 1350 °C due to the decomposition of anhydrous calcium sulfate (anhydrite).

These results are very different in EF (Figure 11). After 30 minutes of testing, all the gypsum originally present in the specimen had been decomposed as the loss of crystallization water from gypsum ($\text{CaSO}_4 \cdot 2\text{H}_2\text{O}$) and bassanite ($\text{CaSO}_4 \cdot \frac{1}{2}\text{H}_2\text{O}$) disappears. Therefore, the XRD and TG results confirm a practically quantitative transformation of the totally or partially hydrated phases of calcium sulfate into anhydrite (CaSO_4).

Small differences were found in the CO_2 mass loss associated with carbonates. The specimen least affected by exposure to direct fire was 0.4 w/g since the loss of CO_2 was 1.46% which was higher than that detected in the 0.7 w/g and 0.4 w/g samples with added citric acid (0.64% and 0.34%, respectively). It is important to emphasize that on the face exposed to the fire, the sensors recorded temperatures at around 800 °C. Therefore, the duration of the experiment was prolonged by exposing the coating for 30 minutes to temperatures high enough to partially decarbonate the carbonates and even eliminate them in their entirety. Differences in the compactness and microstructure of the coatings may explain the differences observed in the thermograms of Figure 11. However, the 0.4 w/g originally contained the highest amount of $\text{CaSO}_4 \cdot 2\text{H}_2\text{O}$, which is the mineral that offered the greatest resistance to increased temperatures. This fact may be the key to delaying the destruction of carbonates and explain the higher concentration of calcite in the 0.4 w/g specimen.

4. CONCLUSIONS

1. When citric acid was used, slightly higher temperatures were recorded in the area of direct exposure to fire than when the additive was not used for the same w/g ratio.

2. On the face exposed to fire (EF) there were fewer but thicker cracks in the coatings made with citric acid. Whether or not citric acid was used, the cracks were clearly concentrated in the area exposed to fire. Therefore, such cracks may be related not only to the expansion and contraction processes (thermal stress) that the material may suffer in a fire, but also to substantial modifications of the coating composition.

3. The XRD tests performed on the face not directly exposed to fire (NEF) confirmed that at a depth of 2 cm from the surface of the coating, the material retained a large part of the minerals originally present. However, the first symptoms of gypsum dehydration due to the formation of bassanite ($\text{CaSO}_4 \cdot \frac{1}{2}\text{H}_2\text{O}$) at the expense of gypsum ($\text{CaSO}_4 \cdot 2\text{H}_2\text{O}$) were evident.

4. From a practical point of view, the experimental results indicate that a 2 cm thick gypsum coatings provides a quite effective protection against fire, taking into account the high temperatures reached on the exposed face (around 800 °C). The integrity of the material was confirmed not only by temperature measurements but also from the relatively high concentration of hydrated minerals such as gypsum and bassanite.

5. In general, all the studies carried out by SEM, DRX and TG confirmed that fire has a greater effect on gypsum containing citric acid. In the absence of citric acid, better the behavior against fire is better as it does not inhibit the formation of the mineral $\text{CaSO}_4 \cdot 2\text{H}_2\text{O}$. The evaporation of the crystallization water of this mineral delays the increase in temperature of the sample and, with it, the destruction of other mineral phases of the coating, which may influence the behavior of gypsum coatings for passive protection of other construction and structural elements.

REFERENCES

1. Ministerio de Fomento (2019) Código Técnico de la Edificación. Documento Básico Seguridad en caso de incendio. [En línea]. Available: <https://www.codigotecnico.org/images/stories/pdf/seguridadIncendio/DccSI.pdf>.
2. Gibaru, J. (1965) Enlucidos y revestimientos en la lucha contra los incendios (el yeso). *Mater. Construcc.* 15 [117], 53-67. <https://doi.org/10.3989/mc.1965.v15.i117.1769>.
3. West, R.; Sutton, W.J. (1954) Thermography of gypsum. *J. Am. Ceram. Soc.* 37 [5], 221-224. <https://doi.org/10.1111/j.1151-2916.1954.tb14027.x>.
4. Khalil, A.A.; Hussein, A.T.; Gad, G.M. (1971) On the thermochemistry of gypsum. *J. Appl. Chem. Biotech.* 21 [11], 314-316. <https://doi.org/10.1002/jctb.5020211102>.
5. Ryan, J.V. (1962) Study of gypsum plasters exposed to fire. *J. Res. Natio. Bur. Stand. Sect. C: Eng. Instrum.* 66C [4], 373-394.
6. Karni, J.; Karni, E. (1995) Gypsum in construction: origin and properties. *Mater. Struct.* 28 [2], 92-100. <https://doi.org/10.1007/BF02473176>.

7. Doleželová, M.; Scheinherrová, L.; Krejssová, J.; Vimmrová, A. (2018) Effect of high temperatures on gypsum-based composites. *Constr. Build. Mater.* 168, 82-90. <https://doi.org/10.1016/j.conbuildmat.2018.02.101>.
8. Mehaffey, J. R.; Cuerrier, P.; Carisse, G. (1994) A model for predicting heat transfer through gypsum-board/wood-stud walls exposed to fire. *Fire Mater.* 18 [5], 297-305. <https://doi.org/10.1002/fam.810180505>.
9. Thomas, G. (2002) Thermal properties of gypsum plasterboard at high temperatures. *Fire Mater.* 26 [1], 37-45. <https://doi.org/10.1002/fam.786>.
10. Kontogeorgos D.A.; Founti, M.A. (2012) Gypsum board reaction kinetics at elevated temperatures. *Thermochim. Acta.* 529, 6-13. <https://doi.org/10.1016/j.tca.2011.11.014>.
11. Park, S-H.; Manzello, S.L.; Bentz D.P.; Mizukami, T. (2010) Determining thermal properties of gypsum board at elevated temperatures. *Fire Mater.* 34 [5], 237-250. <https://doi.org/10.1002/fam.1017>.
12. Lázaro, D.; Puente, E.; Lázaro, M.; Lázaro, P.G.; Peña, J. (2015) Thermal modelling of gypsum plasterboard assemblies exposed to standard fire tests. *Fire Mater.* 40 [4], 568-585. <https://doi.org/10.1002/fam.2311>.
13. Weber, B. (2012) Heat transfer mechanisms and models for a gypsum board exposed to fire. *Int. J. Heat Mass Transfer.* 55 [5-6], 1661-1678. <https://doi.org/10.1016/j.ijheatmasstransfer.2011.11.022>.
14. Du, Z.; She, W.; Zuo, W.; Hong, J.; Zhang, Y.; Miao C. (2020) Foamed gypsum composite with heat-resistant admixture under high temperature: Mechanical, thermal and deformation performances. *Cem. Concr. Comp.* 108, 103549. <https://doi.org/10.1016/j.cemconcomp.2020.103549>.
15. Alameda, L.; Calderón, V.; Junco, C.; Rodríguez, A.; Gadea, J.; Gutiérrez-González, S. (2016) Characterization of gypsum plasterboard with polyurethane foam waste reinforced with polypropylene fibers. *Mater. Construcc.* 66 [324], e100. <https://doi.org/10.3989/mc.2016.06015>.
16. UNE-EN 1363-1 (2015) Ensayos de resistencia al fuego. Parte 1: Requisitos generales, AENOR.
17. Moneo, L. (2014) Tesis Doctoral. Protección de recipientes de gases licuados y/o hidrocarburos con revestimiento de morteros modificados para evitar fenómeno de bleve, Elche: Universidad Miguel Hernández. Escuela Politécnica Superior de Orihuela.
18. Luna-Galiano, Y.; Cornejo, A.; Leiva, C.; Vilches, L.F.; Fernández-Pereira, C. (2015) Properties of fly ash and metakaolin based geopolymer panels under fire resistance tests. *Mater. Construcc.* 65 [319], e059. <https://doi.org/10.3989/mc.2015.06114>.
19. Nguyen, Q.T.; Ngo, T.; Tran, P.; Mendis, P.; Aye, L.; Kristombu Baduge, S. (2018) Fire resistance of a prefabricated bushfire bunker using aerated concrete panels. *Constr. Build. Mater.* 174, 410-420. <https://doi.org/10.1016/j.conbuildmat.2018.04.065>.
20. Correia, J.R.; Branco, F.A.; Ferreira, J.G.; Bai, Y.; Keller, T. (2010) Fire protection systems for building floors made of pultruded GFRP profiles: Part 1: Experimental investigations. *Com.: Part B. Engi.* 41 [8], 617-629. <https://doi.org/10.1016/j.compositesb.2010.09.018>.
21. Hurlbut, C.; Klein, C. (1898) Manual de Mineralogía de Dana, Reverté.
22. Badens, E.; Veessler, S.; Boistelle, R. (1999) Crystallization of gypsum from hemihydrate in presence of additives. *J. Cryst. Growth.* 198-199 [1], 704-709. [https://doi.org/10.1016/S0022-0248\(98\)01206-8](https://doi.org/10.1016/S0022-0248(98)01206-8).
23. Lanzón, M.; García-Ruiz, P.A. (2012) Effect of citric acid on setting inhibition and mechanical properties of gypsum building plasters. *Constr. Build. Mater.* 28 [1], 506-511. <https://doi.org/10.1016/j.conbuildmat.2011.06.072>.
24. Singh, N.B.; Middendorf, B. (2007) Calcium sulphate hemihydrate hydration leading to gypsum crystallization. *Prog. Cryst. Growth Charact. Mater.* 53 [1], 57-77. <https://doi.org/10.1016/j.pcrysgrow.2007.01.002>.
25. Magallanes-Rivera, R.X.; Escalante-García, J.I.; Gorokhovskiy, A. (2009) Hydration reactions and microstructural characteristics of hemihydrate with citric and malic acid. *Constr. Build. Mater.* 23 [3], 1298-1305. <https://doi.org/10.1016/j.conbuildmat.2008.07.022>.
26. Vellmer, C.; Middendorf, B.; Singh, N.B. (2006) Hydration of alpha-hemihydrate in the presence of carboxylic acids. *J. Therm. Anal. Calorim.* 86, 721-726. <https://doi.org/10.1007/s10973-005-7224-4>.
27. UNE-EN 13279-1 (2009) Yesos de construcción y conglomerantes a base de yeso para la construcción. Parte 1: Definiciones y especificaciones, AENOR.
28. UNE-EN 13279-2 (2014) Yesos de construcción y conglomerantes a base de yeso para la construcción. Parte 2: Métodos de ensayo, AENOR.
29. Boisvert, J-P.; Domenech, M.; Foissy, A.; Persello, J.; Mutin, J-C. (2000) Hydration of calcium sulfate hemihydrate (CaSO₄·½H₂O) into gypsum (CaSO₄·2H₂O). The influence of the sodium poly(acrylate)/surface interaction and molecular weight. *J. Cryst. Growth.* 220 [4], 579-591. [https://doi.org/10.1016/S0022-0248\(00\)00865-4](https://doi.org/10.1016/S0022-0248(00)00865-4).
30. Inoue, M.; Hirasawa, I. (2013) The relationship between crystal morphology and XRD peak intensity on CaSO₄·2H₂O. *J. Cryst. Growth.* 380, 169-175. <https://doi.org/10.1016/j.jcrysgro.2013.06.017>.
31. Gutiérrez-González, S.; Gadea, J.; Rodríguez, A.; Junco, C.; Calderón, V. (2012) Lightweight plaster materials with enhanced thermal properties made with polyurethane foam wastes. *Constr. Build. Mater.* 28 [1], 653-658. <https://doi.org/10.1016/j.conbuildmat.2011.10.055>.